Materials Science & Engineering B 261 (2020) 114718

Contents lists available at ScienceDirect

Materials Science & Engineering B

journal homepage: www.elsevier.com/locate/mseb

Design of the high performance microbattery with silicene anode

Alexander Y. Galashev*, Andrey V. Suzdaltsev, Ksenia A. Ivanichkina

Institute of High-Temperature Electrochemistry UB RAS, Yekaterinburg, Russia
Ural Federal University, Yekaterinburg, Russia

ARTICLE INFO

Keywords:
Cathode
Design
Graphite
Lithium ion battery
Si-based anode
Silicene

ABSTRACT

To date, lithium-ion batteries have become one of the most important energy storage devices. Creating lithium ion microbatteries using materials structured at the nanoscale allow you to create solid-state lithium-ion batteries that have the fastest electrodes. In this work, we propose the design of an element of a lithium-ion current source, which has a 10 times higher stored energy density than similar devices that are widely used at present. The developed electrochemical cell has a fully solid-state design. The active material of the anode is silicene, a solid-state electrolyte is used, the cathode is made of complex transition metal oxides, and an ultra-thin insulating pad is used. The presented element of the secondary lithium-ion battery has a theoretical capacity of 3500 mAh g^{-1} and a high charging speed. The electrochemical cell is characterized by small size, low cost of components and operational safety.

1. Introduction

On the way to creating personalized medical devices and ones for intellectual linking of various biological organs, modern medicine needs flexible, high-performance solid state microbatteries. Such batteries are a major factor affecting the total weight and size of any implantable and wearable devices. In particular, the need for radical changes is seen in the use of potentially damaging orthodontic applications. Of course, every implantable device must pass a toxicity test before it is used. Following the integration strategy, implantable flexible electronic components should be equipped with a flexible battery or even a battery module. Such a module can be created, for example, by transferring several batteries to polyethylene terephthalate and their connection using a composite material based on aluminum. Furthermore, flat-panel printed micro-batteries without separators can be designed for micro-level applications.

The disadvantage of modern batteries is their relatively low capacity, high weight and low charging speed [1]. It is possible to increase the productivity and efficiency of this electrochemical device by using new materials in its design. The main functional parts of the battery are the cathode, anode, electrolyte and separator, which passes the desired ions in a given direction. As the active material of the cathode of lithium ion batteries (LIBs), lithiated cobalt, nickel and manganese oxides are intensively used. The use of nanomaterials with a small particle size and a more uniform distribution of their size can improve the electrochemical characteristics of the cathode material. A cathode material is also created based on the lithium-iron phosphate compound $LiFePO_4$ having an olivine structure.

The anode material is mainly graphite and other carbon materials; in particular, a mixture of graphite or graphite materials with “soft” or “hard” disordered carbons. Recently, one is increasingly resorting to the use of carbon nanotubes (CNTs) when designing the anode of a lithium battery. The disadvantage of carbon anodes is their low capacity, the theoretical value of which is only 372 mAh g^{-1} [2]. Anode materials must have high characteristics of specific capacitance, be safe during operation, give high current densities and have a low price. Such materials include silicon, tin, their compounds, transition metal nitrides, as well as composites including these materials. As is known, silicon is characterized by a high theoretical specific capacity (4200 mAh g^{-1}) and can be considered as the main candidate for use as an anode material in LIBs [3]. However, crystalline silicon has a strong change in volume during cycling, as a result of which it is rapidly destroyed. The transition to thin-film silicon anodes avoids this drawback, but another difficulty appears.

Thin-film silicon anodes have a relatively large capacity loss during the charge-discharge process. However, the stability of this process increases significantly with decreasing thickness of the silicon film. Thin film anodes based on SnO_2 have a rather high capacity (~700 mAh g^{-1}) and good stability during the charge – discharge process [4]. However, during the first cathodic polarization, a significant amount of electricity is expended on an irreversible capacity.

The standard liquid electrolyte is a 1 M solution of $LiPF_6$ in a

* Corresponding author at: Institute of High-Temperature Electrochemistry UB RAS, Yekaterinburg, Russia.
E-mail address: galashev@ihte.uran.ru (A.Y. Galashev).

https://doi.org/10.1016/j.mseb.2020.114718
Received 8 May 2020; Accepted 14 August 2020
Available online 09 September 2020

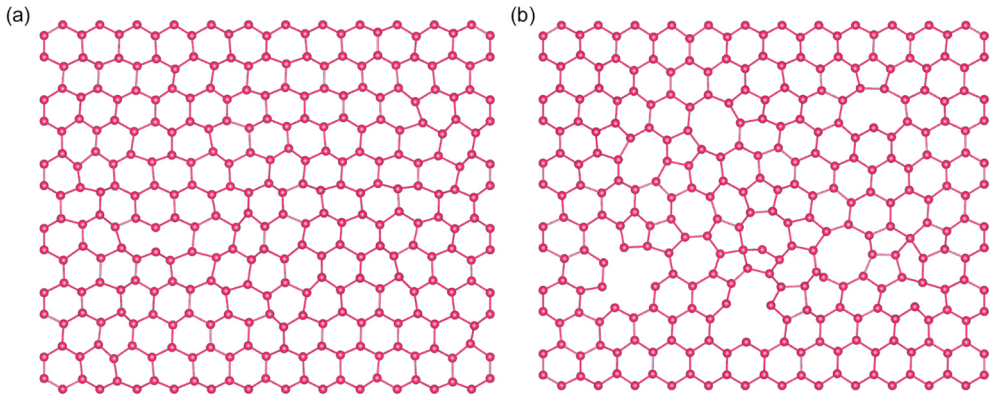

Fig. 1. *Xy* silicene sheet projection, after lithiation process (after 50 ps): (a) silicene on graphite substrate; (b) silicene on Ag(1 1 1) substrate.

mixture of ethylene carbonate and dimethyl carbonate. The battery can be made fully solid state. In a thin-film battery, a solid inorganic electrolyte of the composition $Li_{3,6}Si_{0,6}PO_4$ can be used. At present, LiPON is often offered as an electrolyte for thin-film batteries. The conductivity of LiPON at room temperature is almost two orders of magnitude lower than that of conventional liquid electrolytes. However, its integral resistance is acceptable for a typical electrolyte thickness of the order of 1 μm.

The separator separates the positive and negative electrodes inside the LIB and serves to prevent short circuits. Below a temperature of 130 °C, LIB can use a polyethylene separator, or, for example, a polypropylene separator with a polymer binder composite and cerium oxide nanoparticles deposited on it.

After a large number of charge and discharge cycles, lithium dendrites appear in the LIB with liquid electrolyte. They shorten battery life, cause a point rise in temperature and short circuits. Moreover, dendrites can grow so much that they destroy the battery cells, causing an explosive chemical reaction between the electrodes and the electrolyte.

A new polymer electrolyte for electrical double layer capacitor containing alkali metal salts and ionic liquid to facilitate ion diffusion was investigated in a temperature range of 30–120 °C [5]. The creation of hybrid superacapacitors or "supercapattery" allows you to extract good values of the specific power and energy from the same device. Polypyrrole (PPy) in combination with a classic battery electrode can improve the specific power of an element while maintaining good specific energy. For this, in a battery based on an aqueous electrolyte, for example, a PPy electrode connects to a zinc or lead-sulfate anode [6].

Solid polymer electrolytes have a temperature limitation on the mobility of cations, so that their real ionic conductivity is from 10^{-3} to 10^{-5} S · cm^{-1} [7,8]. A solid electrolyte in the form of an acicular crystalline organoboron compound was proposed in works [9,10]. The conduction mechanism is based on the interaction of the organoboron compound with the anion of the Li salt. A large path of lithium ions is created due to the corresponding structural orientation. The maximum ionic conductivity (2.7–7.1) × 10^{-4} S · cm^{-1} is reached on a range of 30–60 °C.

So far, fully solid-state low-temperature batteries are under development. For example, a battery was tested with lithium metal as the anode and $LiFePO_4$ as the cathode [9]. A low-temperature solid electrolyte can be made on the basis of starch, the monomer of which contains two -O-C-O- bonds, which promote the dissociation of lithium salt [11]. A battery with such an electrolyte is capable of discharging not only at room temperature, but also at −20 °C. At room temperature, the average ionic conductivity of the electrolyte was 3.10 × 10^{-4} S · cm^{-1}. However, the average discharge capacity of the battery, obtained during 200 cycles, was only ~114 mA h g^{-1}. The main factor in reducing the LIB performance when the temperature is lowered to −10 °C is high charge transfer resistance R_{ct}. The main contribution to the increase in R_{ct} is made by the anode (graphite) and cathode [12]. The use of traditional electrodes also creates the problem of rapidly reducing the charge storage capacity with increasing charge/discharge rate [13]. At the same time, the amount of energy delivered at high power is reduced. Ways to solve the problem are reducing the thickness of the electrode [14], enhancing solid-state diffusion [15], increasing the porosity of the electrode [16], etc.

This article discusses the new design of the miniature LIB element, on the basis of which it is possible to achieve very high energy consumption and LIB power with stable security.

2. Materials and methods

In a typical LIB, energy is released during the transfer of lithium ions between two electrodes – an anode and a cathode, with a cathode typically comprising lithium and transition metals such as cobalt, nickel and manganese. The ions flow between the electrodes through a liquid electrolyte.

The designs of electrochemical cells shown in Figs. 1 and 2, we have developed on the basis of both first-principle and classical molecular dynamics calculations [17,18]. The use of a graphite substrate for

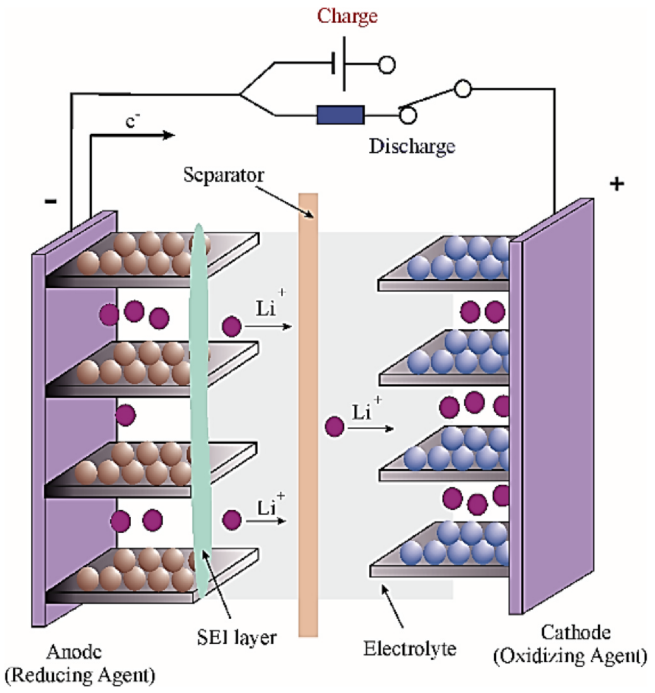

Fig. 2. Schematic diagram of LIB with liquid electrolyte.

Table 1
Adhesion energies between the metal substrate and the perfect silicene sheet, the bond length between the atoms in the substrates and the total charge of silicene.

Property	Al	Ni	Cu	Ag
E_{adh}, eV	0.341	0.898	0.852	0.414
Me-Me, Å	2.896	2.492	2.629	2.919
Q_v, a.u.	−0.339	−1.412	−0.955	−0.955

silicene leads to a significantly larger capacity of the electrochemical cell than the use of metal (Ag, Al, Cu, and Ni) substrates for this purpose [19,20]. Table 1 shows the values of the adhesion energy between the metal substrate and the sheet of silicene (E_{adh}), the bond lengths between the metal atoms in the substrates and the total electric charge Q_v, which silicene acquired from the substrate when the number of Si atoms and the metal substrate was 1: 2.67. The charge calculation Q_v was based on the estimation of the elementary charge of the atoms of the system by the method proposed in [21]. This method uses the partition of the space occupied by atoms into sections using Voronoi polyhedra. Then, the charge density ρ, corresponding to this part of space is taken into account as the charge for the atom.

The adhesion energy E_{adh} between silicene and graphite (0.03 eV/atom) is significantly lower than that between silicene and the metals we have examined [22]. Low values of E_{adh} contribute to the preservation of the remarkable physical properties of silicene, including ensuring the effective functioning of the anode. The largest negative charge is transferred from the Ni substrate to silicene and the adhesion energy in this case is the largest. The lowest charge is transferred to silicene from the Al substrate at the minimum adhesion energy among presented in Table 1.

Below are the results of the lithium intercalation process into the two-layered silicene channel obtained by molecular dynamics (MD) modeling. The Fig. 1 shows the snapshot of sheet of silicene directly adjacent to the substrate at the final stage of the intercalation process in the two-layered silicene channel placed on the graphite (Fig. 1a) and Ag (1 1 1) (Fig. 1b) substrate (lithium is not shown in the figure). It can be seen that silicene located on a silver substrate is more impressible to destruction. This result is a consequence of the silicene high adhesion energy to the metal substrate.

3. Results and discussion

3.1. Design of the electrochemical cell

Schematic diagram of LIB with liquid electrolyte is shown in Fig. 2. The space between the cathode and the anode is filled with liquid electrolyte. A separator is placed in the liquid electrolyte, separating the cathode and anode parts of the battery and preventing it from short circuiting. So far, it has not been possible to solve the problem of the formation of a solid electrolyte interphase (SEI). Typically, the SEI layer results from the decomposition of organic and inorganic compounds. This occurs mainly after the first charge/discharge cycle. SEI contains electrolyte and active material (lithium) components.

The degradation of a cathode made of layered transition metal oxides, such as $LiCoO_2$, occurs due to fatigue and its loss of free lithium. The associated decrease in capacity can be slowed down by using anodes with stable potential and/or anodes containing lithium. To eliminate adverse reactions at the electrode/electrolyte interface, suitable solid-state electrolytes can be used [23].

When using liquid electrolyte, the mechanical load during cycling can completely break the separator if it was previously damaged. A short circuit that occurs inside the cell creates very high currents and causes the cell to overheat. The critical temperature is T = 200–220 °C. At such temperatures, pressure rises, the cell breaks down, and the electrolyte filling it enters into reactions, releasing volatile substances.

In this case, the electrode material decomposes, and as a result of the reaction, hydrogen is released, which ignites from the spark. One of the methods for solving this problem is the use of solid electrolytes. Their variety is electrolytes, consisting of polymer chains forming a rubbery lithium conductor. This method inhibits the growth of dendrites. However, such complex materials cannot recover from damage. Many modern solid electrolytes withstand the mechanical stresses that appear during cycling, do not allow dendrites to grow, and thereby largely solve the LIB safety problem.

The schematic diagram of the electrochemical cell under

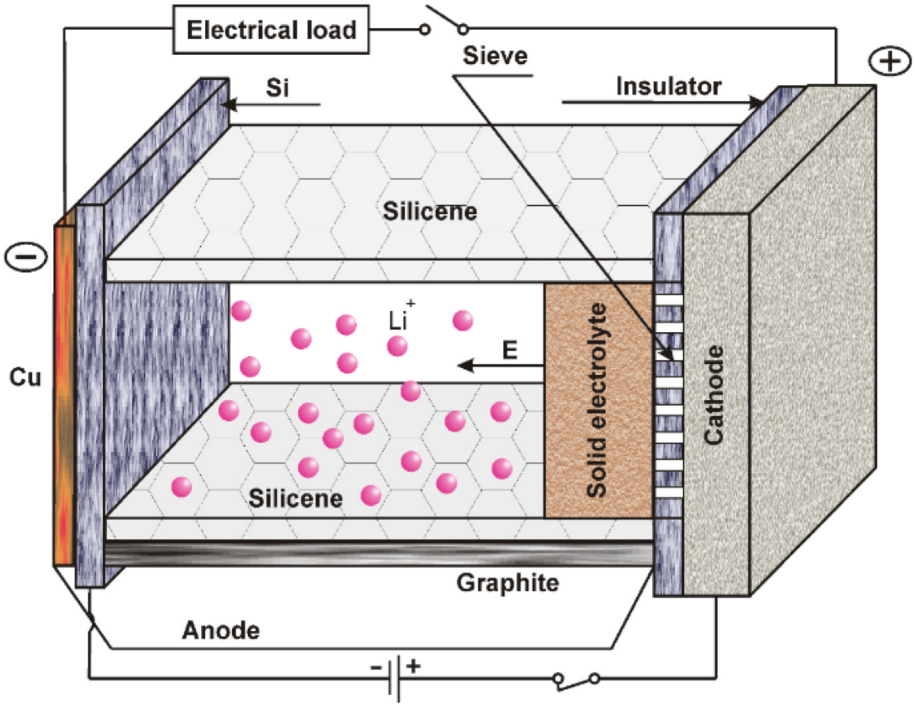

Fig. 3. Schematic diagram of the cell lithium-ion battery with a silicene anode.

consideration is shown in Fig. 3. The LIB element is a fully solid. The anode part of the element consists of a copper current collector, a silicon film deposited on it and perpendicular to it sheets of silicene, one of which is on a graphite substrate. Both sheets of silicene are bonded to a nanostructured silicon film by electrical discharge. Between the sheets of silicene is a solid electrolyte, which through a molecular sieve is in contact with the cathode. In a solid state battery, the separator can be an order of magnitude thinner (3–4 μm) than in a "traditional" lithium battery, or completely absent. Between sheets of silicene, including a sheet located on a graphite substrate, and the cathode, an insulating film is located, at the site of contact of which with the electrolyte a molecular sieve is created. The sieve allows lithium ions to pass from the solid electrolyte to the cathode and vice versa. When the cell is charged, Li^+ ions under the influence of a constant electric field exit the electrolyte and rush mainly towards the film of nanostructured silicene. Due to the movement along the lines of the electric field directed towards the silicene sheets, as well as in collisions, they lose energy and are deposited on the surface of silicene, and at high density they also fill the central part of the silicene channel. Some ions are deposited on a nanostructured silicon surface. Such a movement makes it possible to fill the silicene channel with Li^+ ions as densely as possible. When the battery is discharged, lithium ions move in the opposite direction.

Thin-film solid electrolytes can be used in the cell - the so-called antiperovskites, for example, Li_3OCl, Li_3OBr and $Li_3OCl_{0.5}Br_{0.5}$, which demonstrate high stability during cycling. Electrolytes with a garnet-like structure: $Li_5La_3Ta_2O_{12}$, $Li_5La_3Nb_2O_{12}$ as well as sulfide type Li-ion conductors: $Li_{10}GeP_2S_{12}$, $Li_2Sn_2S_5$ and others have high electrical conductivity. Types of solid-state electrolytes and the prospects for their use are well discussed [24]. The electrolyte is in a bound state. High electrical conductivity is one of the main requirements for such an electrolyte. The main strategies for increasing the ionic conductivity of solid electrolytes are described in Ref. [24]. This battery is the most environmentally friendly and practical in all respects. It has the highest level of energy intensity. A schematic diagram of an electrochemical cell for a secondary LIB is shown in Fig. 2. The anode (left) contains a current collector (thin copper film), an insulator, and two sheets of silicene, one of which is located on a graphite substrate. Due to the close density of graphite and silicon, the main factor affecting the specific capacitance of the electrode will be a significantly higher adsorption capacity of silicene. Therefore, the graphite substrate should be as thin as possible.

In this design, the substrate and the sheets of silicene belonging to the anode are isolated from the cathode. The upper silicene sheet does not have a graphite substrate, which allows both sides of this sheet to be used in the construction of the LIB. LIB can be obtained by joining in the vertical direction of such cells. It is more advantageous to connect mirror elements (relative to a plane parallel to the plane of silicene). In this case, in principle, for two sheets of silicene (without support), each of the surfaces can be used for lithium adsorption. Silicene sheets are separated by a gap of 0.24–0.75 nm using a solid electrolyte (right). The value of $h_g = 0.24$ nm was determined in the DFT calculations as a gap in a two-layer freestanding silicone [25]. To study lithium intercalation/deintercalation in a silicene channel on metal substrates, a gap of $h_g = 0.75$ nm was used [26–28]. On the left, the sheets of silicene rest on a film of silicon deposited on a copper foil. The cathode (right) is in direct contact with solid electrolyte only. When charging the battery, Li^+ ions fill the silicene channel (anode element), and when discharged through a solid electrolyte, they partially return to the cathode. The main features of the electrolyte are the higher ionic conductivity and high electrical resistivity. The cathode can be made of $LiCoO_2$, ZrO_2, Al_2O_3, Li_3PO_4, $LiNbO_3$, $LiTaO_3$ and many other materials. High-energy cathodes with high chemical resistance for LIBs are discussed earlier [29]. External electrical circuits are conventionally shown. A battery discharge is accompanied by a decrease in voltage between its electrodes.

3.2. The implementation of the design of the electrochemical cell

Silicene on a graphite substrate was obtained experimentally by direct deposition of silicon on a chemically inert graphite substrate at room temperature [30]. Highly oriented pyrolytic graphite (HOPG) 12 × 12 × 1 (mm) in size was used as a substrate. A fresh graphite surface was obtained by peeling off the HOPG substrate with tape in a nitrogen atmosphere, and then transferred to an ultra-high vacuum (UHV) chamber. High-purity silicon (Sil'tronix ST, $\rho = 10^{-9}$ Ohm × cm) was evaporated from a tungsten crucible in the form of a basket located 200 mm from the substrate. The deposition was carried out under ultra-low pressure (10^{-10} Torr) with a constant speed of 0.01 nm/min (0.04 ml min^{-1}) at room temperature. Due to the specific nature of the HOPG substrate, which is formed by large and very flat single crystals disoriented in the basal plane with respect to each other around the growth axis (0001), it was not possible to perform reliable low-energy electron diffraction studies. The diffraction pattern was formed by a series of continuous circles with some spots reflecting the crystal structure of each graphite single crystal. Using the scanning tunneling spectroscopy and calculation of the band structure, the metallic character of the deposited silicene was shown. DFT calculations also reflect the presence of the Dirac cone. The size of the grown homogeneous silicene structure was approximately 2 × 2 (μm).

A porous Si/copper film with a large surface area can be fabricated, for example, by electrodeposition [31]. In addition, nanostructured silicon can be deposited on copper foil, which serves as a current collector in LIB. You can use copper foil with a thickness of 50 nm and even 20 nm. In this case, the adhesion between copper and silicon must be reliable. For this, a film with a thickness of ~100 nm, consisting of Ti-W (90%/10%) Ta, or TiN is deposited and serves as a bonding agent for adhesive purposes between the silicon film and the current collector copper foil. This minimizes the dissolution of copper and the formation of dendrites.

Silicene does not exist in nature as a three-dimensional material, because silicon atoms prefer sp^3- rather than sp^2 hybridization. This makes the synthesis of free-standing silicene very difficult, if not impossible. However, by epitaxial growth of silicene, it is possible to obtain it on metal substrates, and then use the outstanding properties of this material by transferring it to an insulating substrate [32]. In addition, calculations from first principles show that the interaction of silicene grown on hexagonal boron nitride with a substrate is very small. As a result, quasi-free-standing silicene is realized on this substrate [33].

Defects in single-layer materials in the form of vacancies are easily induced by laser radiation or an electron beam. They are almost inevitable in the manufacture and processing of monolayers. Sometimes small defects are introduced purposefully for specific applications [34]. For example, two-dimensional materials with defects are an excellent membrane for gas separation [35].

The connection of sheets of silicene with nanostructured silicon deposited on a copper foil can be carried out using an electric discharge using a technology similar to splicing of optical fibers [36].

The 2 μm thick Li_3OCl film used as an electrolyte demonstrates excellent stability and compatibility with metallic Li [37]. Anti-perovskite Li_3OCl films with increased ionic conductivity are deposited by pulsed laser deposition at temperatures below 300 °C. It was found that the ionic conductivity of the Li_3OCl films is $8.9 \cdot 10^{-6}$ Cm cm^{-1} at room temperature and $3.5 \cdot 10^{-4}$ Cm cm^{-1} at 140 °C.

As a flexible insulator, an organic polymer poly (1,3,5-trimethyl-1,3,5-trivinylcyclotrisiloxane) (pV3D3) can be used. It is obtained by the method of initiated chemical vapor deposition (iCVD) [38]. Gaseous monomers in a high vacuum react with polymerization initiators. As a result, ultrathin (~8 nm) polymer films are formed on the substrate. Uniform and pure ultrathin pV3D3 films with excellent insulating properties, have a very large band gap (> 8 eV) and tensile strain resistance of up to 4%. In the absence of solvent, the iCVD process allows

conformally growing pV3D3 on plastic substrates, as well as on various channel layers, including organics, oxides, and graphene.

The insulating pad separating the anode from the cathode is made of an ultrathin pV3D3 film, on which holes are punched at the junction of the solid electrolyte with the cathode using ion bombardment. A sieve in the insulating pad between the electrolyte and the cathode allows Li^+ ions to flow from the electrolyte to the cathode in the discharge mode and back when charging.

3.3. A specific example of the design of an electrochemical cell

Freestanding silicene is a narrow-gap semiconductor with a direct band gap of about 0.15 meV [39]. It was found that when silicene forms on graphite, the band gap increases to about 37 meV and becomes quite comparable with the band gap of silicene on graphene (57 meV) [40]. The low electrical conductivity of this material should manifest itself in a low rate of charging and discharging LIB. However, silicene on the substrate can significantly change its electronic properties, including becoming a conductive material [3].

The theoretical electric capacity (*EC*) of the material "silicene on graphite" in mAh g^{-1} can be calculated as [41]:

$$EC = \frac{n_{Li}F}{3.6(n_C m_C + n_{Si} m_{Si})} \quad (1)$$

where m_{Si} and m_C are the masses of silicon (Si) and carbon atoms (C); n_{Li}, n_{Si} and n_C are the number of Li, Si and C atoms in the supercell, respectively; F - Faraday constant, $F = 96\,486.7$ C mol^{-1}.

It is possible to estimate the capacity of the silicene layer on graphite, taking into account the fact that for the actually obtained silicene and graphene at 2 nm^2 there is 1 vacancy type defect (mono- or bivacancy) [3]. It is reasonable to assume that a maximum of 4 top layers can be active in graphite, i.e. lithium ions that have passed through defective silicene can drop to this level. It is this number of graphite layers that can be limited to obtain a one-sided Si-C layer. For double-sided graphite coating with silicene (Si-C-Si), eight-layer graphite can be used. Then the composition of SiC_7 will approximately describe the ratio between the atoms of the active layers of silicene and graphite. The initial coating of silicene with one layer of Li atoms corresponds to the loading of 16 Li per supercell. Then, in accordance with (1), the active material SiC_7 corresponds to a capacity of 955.84 mA h g^{-1}, which is more than 2.5 times the capacity of graphite. If for each Si-C layer, in addition to one layer located on graphite, there will be 1, 2, 3, 4 ones having 2 working surfaces, then the total capacity of the obtained LIB element will be 2577, 3118, 3388 and 3551 mAh g^{-1}, respectively. Already with one additional layer of silicene, an electrode capacity of almost 7 times higher than that of graphite will be achieved. The active part of the anode element with a capacity of at least 3500 mAh g^{-1} is shown in Fig. 4.

One layer of silicene binds to the graphene layer (one layer of graphite) with an adhesion energy of about 0.025 eV/atom [42]. This energy is significantly lower than the adhesion energy between the metal substrate and the perfect silicene sheet: 0.89, 0.41, 0.85, and 0.34 eV/atom for the (Ni, Ag, Cu, and Al) (1 1 1) substrates, respectively. A graphite substrate cannot significantly change the physical properties of free-standing silicene. Thus, such a substrate in contact with silicene can successfully participate in intercalation/deintercalation of lithium.

The actual charge capacity of a silicene electrode may decrease due to the onset of mechanical instability. So, for a duo-layer silicene in the absence of a substrate, the capacitance can drop to 1384 mA·h g^{-1} [22]. However, this value is still more than 3 times higher than the corresponding theoretical characteristic of the currently functioning LIBs. The high performance of microbatteries is made possible by a sharp reduction in the thickness of their electrodes and electrolyte, which reduces the diffusion path of ions by orders of magnitude. In addition, ions in such super thin batteries, turn out to be significantly faster due to a significant increase in the electric field strength. The field strength increases greatly due to the small thickness of the used film materials. Therefore, the force pushing the ions in the direction of the electric field increases significantly. The microbatteries discussed here will be fully functional even at room temperature.

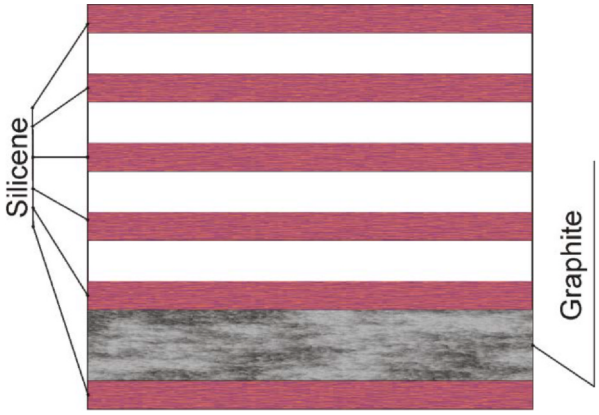

Fig. 4. The active material of the multilayer silicene element for the anode with a capacity of at least 3500 mAh g^{-1}.

The lithium diffusion coefficient (*D*) calculated by the molecular dynamics method and averaged over the channel gap for the unirradiated and irradiated (transmutation neutron doped) systems is 1.25×10^{-5} cm^2 s^{-1} and 1.69×10^{-5} cm^2 s^{-1}, respectively. This is only 5.4 and 4.0 times less than the self-diffusion coefficient of liquid lithium at the melting point ($6.8 \pm 0.3 \times 10^{-5}$ cm^2 s^{-1}) [43]. The battery charging rate is already considered acceptable when the diffusion coefficient of ions *D* in the anode is in the range from 10^{-10} to 10^{-13} cm^2 s^{-1} [44]. The values of the coefficient *D* achieved in our model can provide e a very high speed of charging the battery.

As component materials for a unit cell of a lithium-ion current source, the following can be used:

(i) copper foil (industrial production) with a thickness of 20 nm and a width of more than 2n μm as a current collector, where n is the number of strips in the electrodes; the length of the foil is determined by the size of the electrodes (see below);
(ii) nanostructured silicon with 5 sheets of silicene perpendicularly attached thereto, one of which is directly adjacent to the graphite substrate, with a thickness of not more than 8 layers, each silicene sheet has a size of 4 × 2 μm, the graphite substrate has the same horizontal dimensions, the gap between the silicene sheets is 0.75 nm, if they were not subjected to transmutation doping with phosphorus, otherwise the gap can be reduced up to ~0.30 nm;
(iii) the electrical conductivity of Li^+ polycrystals based on Li_3OCl (10^{-4}–10^{-3} S cm^{-1}) is one of the highest reported for crystalline materials. The use of Li_3OCl, Li_3OBr or $Li_3OCl_{0.5}Br_{0.5}$ can significantly increase the electrolyte performance in miniature LIBs, the width of one strip of the electrolyte film is 2 μm, and the length is determined by the height of the unit cell of the lithium-ion current source and the number of such cells; the number of bands in the electrolyte corresponds to that in the LIB electrodes, determined by the power of the created current source;
(iv) a cathode made of lithium cobalt oxide ($LiCoO_2$), can be deposited by radio frequency sputtering [45], the planar dimensions of the cathode correspond to the dimensions of the anode components and similar sizes of the used solid electrolyte;
(v) the insulating strip separating the anode from the cathode is made of an ultra-thin pV3D3 film, the planar dimensions of the strip correspond to that of the electrolyte and cathode.

3.4. Advantages of the proposed LIB design over other designs

A better understanding of the advantages of this anode design is given by comparison with other previously proposed anodes.

Example 1. What happens when instead of silicene, silicon powder (10 mm) is used as an anode component?

When using Si powders as the LIB anode, a large irreversible capacity (2090 mAh g^{-1}) is created during the first cycle, and the number of acceptable cycles is limited to only 10 [46]. In this case, crystalline Si (c-Si) turns into amorphous Si (a-Si). This is due to the formation of the c-$Li_{15}Si_4$ alloy during the first lithiation [47]. Complete introduction of lithium leads to a large change in volume (up to 300%), which will soon cause cracking and grinding of Si active materials [48]. Because of this, there is a gradual loss of electrical contact between the Si and the current collector, and the resulting film of solid SEI leads to a large irreversible capacity and poor cycling performance.

Example 2. The use of other Si nanomaterials as an anode component.

Nanostructured Si materials with a particle size greater than 20 nm are subjected to the same great deformations, stresses (as larger particles), and give a large change in the volume of Si during cycling [49]. However, between them, i.e. inside porous Si there is an empty space that can also accommodate a large amount of lithium. Therefore, various nanostructured Si materials, including zero-dimensional (0D) Si nanoparticles; one-dimensional (1D) Si nanowires, nanorods and nanotubes; two-dimensional (2D) thin films; and a three-dimensional (3D) porous structure can also be used as an anode material to improve cycling [50].

Example 3. The use of a composite matrix in the design of the anode.

To partially remove the stress and increase the electronic conductivity of the Si-based electrode, a composite matrix with high mechanical strength and high conductivity can be used. Such a solution will prevent a decrease in capacity [51]. The composite structure can significantly reduce the contact area between the active materials and the electrolyte. This promotes the formation of a stable SEI layer [52]. Technology for creating MXenes materials uses various matrices (graphite, amorphous carbon, metal, metal oxides) to improve the electrochemical performance of Si-based anodes [53]. The formation of a stable interface between the electrode and the electrolyte and electrode reinforcement is facilitated by the functionalization of groups on the Si surface. Such a procedure gives better bonding and preserves the integrity of the electrode when changing the volume of Si. A good reinforcing material is SiO_x, giving a low volume change during cycling [54]. Despite the fact that using SiO_x a relatively stable cyclic productivity is achieved; the use of this material leads to the formation of silicates Li_2O and lithium. Silicate formation leads to a large irreversible capacity during the first cycle.

Example 4. Anode in the form of a 2D / 3D structure of active materials.

The use of a copper current collector without a binder in the electrode facilitates the transfer of electrons and ions throughout the electrode, improves contact between Si particles and a copper collector, and reduces the likelihood of breaking the connection of electrode particles with an external circuit. For example, a Si/C multilayer film electrode has a good-controlled Si-C interface due to its carbon coating [55]. The active material of the anode in this case are porous Si nanowires that do not have a binder. A properly constructed 3D conductive frame in Si allows you to increase the load density [56]. Improving the mechanical properties of the electrode slows down structural degradation during lithiation/deliteration processes.

Example 5. Anode in the form of a Si particle-graphite composite.

Si particles-graphite can be considered as well suited for next-generation anodes [57]. They have high gravimetric ability, excellent cyclability and are capable of producing high power density. The advantage of this design is that Si particles block the graphite mesopores and prevent cracking of graphite flakes due to the appearance of high stress caused by deformation. In addition, a low voltage is created in the Si layer located in the internal macropores of graphite. All this leads to minimal swelling of the electrode and to excellent stability during cycling. The lithiation and delitiation of the graphite and Si component in graphite composite electrodes during cycling can be observed using x-ray equipment through operand energy [58]. Such a study allows us to optimize the volumetric expansion of Si particles, to determine their required number in mixed electrodes. Thanks to these measures, a significant improvement in cycling, productivity and long-term stability can be achieved.

The design of the electrochemical cell that we presented by the most important characteristics (power, energy intensity, safety) significantly exceeds the designs described in the above examples.

4. Conclusions

We have developed the design of the electrochemical cell, which in its main parameters (capacity, power, safety) is noticeably superior to existing analogues. Based on the union of hundreds or even thousands of such unit cells, a new generation lithium-ion current source can be created many times superior in terms of main parameters to existing LIBs. A comparative analysis of the operational characteristics of the proposed and the most famous to date LIB designs has been carried out. It is shown that the proposed design exceeds the available ones not only in all the main technical indicators, but has flexibility, extremely small dimensions, a very high speed of charging the battery, low price and high explosion safety. The materials necessary for its construction have already been obtained. However, the manufacturing technology of such an anode has not yet been developed. This work can serve as a starting point for the serial creation of the fully safe electrochemical cell presented here and a new anode for the LIB based on it.

Declaration of Competing Interest

The authors declare that they have no known competing financial interests or personal relationships that could have appeared to influence the work reported in this paper.

Acknowledgments

The work was performed within the framework of agreement No. 075-03-2020-582/1 of 18.02.2020 (topic number 0836-2020-0037).

References

[1] A.Y. Galashev, Y.P. Zaikov, New Si–Cu and Si–Ni anode materials for lithium-ion batteries, J. Appl. Elecrtochem. 49 (2019) 1027–1034, https://doi.org/10.1007/s10800-019-01344-9.
[2] A.E. Galashev, Y.P. Zaikov, R.G. Vladykin, Effect of electric field on lithium ion in silicene channel.Computer experiment, Rus. J. Electrochem. 52 (2016) 966–974, https://doi.org/10.1134/S1023193516100049.
[3] A.Y. Galashev, K.A. Ivanichkina, Computational investigation of a promising Si–Cu anode material, PCCP 21 (2019) 12310–12320, https://doi.org/10.1039/c9cp01571j.
[4] L.K. Altunina, L.I. Svarovskaya, O.G. Terekhova, A.A. Magaeva, V.I. Itin, Sorption activity of nanosized powders of SnO2 and CoFe2O4, Chem. Sustain. Dev. 19 (2011) 217–222.
[5] N. Farah, H.M. Ng, A. Numan, C.-W. Liew, N.A.A. Latip, K. Ramesh, S. Ramesh, Solid polymer electrolytes based on poly(vinyl alcohol) incorporated with sodium salt and ionic liquid for electrical double layer capacitor, Mater. Sci. Eng. B 251 (2019) 114468, , https://doi.org/10.1016/j.mseb.2019.114468.
[6] B.N. Grgur, M. Janačković, B.Z. Jugović, M.M. Gvozdenović, The initial characteristics of the polypyrrole based aqueous rechargeablebatteries with supercapattery characteristics, Mater. Sci. Eng. B 243 (2019) 175–182, https://doi.org/10.1016/j.mseb.2019.04.013.
[7] Q. Li, E. Wood, H. Ardebili, Elucidating the mechanisms of ion conductivity

enhancement in polymer nanocomposite electrolytes for lithium ion batteries, Appl. Phys. Lett. 102 (2013) 243903, , https://doi.org/10.1063/1.4809837.
[8] Y.S. Kim, Y.G. Cho, D. Odkhuu, N. Park, H.K. Song, A physical organogel electrolyte: characterized by in situ thermo-irreversible gelation and single-ion-predominent conduction, Sci. Rep. 3 (2013) 1917, https://doi.org/10.1038/srep01917.
[9] P. Joshi, R. Vedarajan, N. Matsumi, A crystalline low molecular weight cyclic organoboron compound for efficient solid state lithium ion transport, Chem. Commun. 51 (2015) 15035–15038, https://doi.org/10.1039/c5cc04753f.
[10] P. Joshi, R. Vedarajan, A. Sheelam, K. Ramanujam, B. Malaman, N. Matsumi, An all solid-state Li ion battery composed of low molecular weight crystalline electrolyte, RSC Adv. 10 (2020) 8780–8789, https://doi.org/10.1039/C9RA09559D.
[11] Z. Lin, J. Liu, Low-temperature all-solid-state lithium-ion batteries based on a di-cross-linked starch solid electrolyte, RSC Adv. 9 (2019) 34601–34606, https://doi.org/10.1039/C9RA07781B.
[12] S. Zhang, K. Xu, R. Jow, The low temperature performance of Li-ion batteries, J. Power Sources 115 (1) (2003) 137–140, https://doi.org/10.1016/S0378-7753(02)00618-3.
[13] R. Tian, S.-H. Park, P.J. King, G. Cunningham, J. Coelho, V. Nicolosi, J.N. Coleman, Quantifying the factors limiting rate performance in battery electrodes, Nat. Commun. 10 (2019) 1933, https://doi.org/10.1038/s41467-019-09792-9.
[14] R. Zhao, S. Zhang, J. Liu, J.J. Gu, A review of thermal performance improving methods of lithium ion battery: electrode modification and thermal management system, J. Power Sources 299 (2015) 557–577, https://doi.org/10.1016/j.jpowsour.2015.09.001.
[15] W.B. Du, A. Gupta, X.C. Zhang, A.M. Sastry, W. Shyy, Effect of cycling rate, particle size and transport properties on lithium-ion cathode performance, Int. J. Heat Mass Transfer 53 (2010) 3552–3561, https://doi.org/10.1016/j.ijheatmasstransfer.2010.04.017.
[16] W. Bauer, D. Notzel, V. Wenzel, H. Nirschl, Influence of dry mixing and distribution of conductive additivesin cathodes for lithium ion batteries, J. Power Sources 288 (2015) 359–367, https://doi.org/10.1016/j.jpowsour.2015.04.081.
[17] A.E. Galashev, K.A. Ivanichkina, Computational study of the properties of silicon thin films on graphite, Rus. J. Phys. Chem. A 91 (12) (2017) 2448–2452, https://doi.org/10.1134/S003602441712007X.
[18] A.E. Galashev, A.S. Vorob'ev, The first principles calculations of the interaction between Li, Na, and K atoms and silicene, Rus. J. Phys. Chem. A 92 (12) (2018) 2513–2517, https://doi.org/10.1134/S0036024418120142.
[19] A. Galashev, K. Ivanichkina, K. Katin, M. Maslov, Computational study of lithium intercalation in silicene channels on a carbon substrate after nuclear transmutation doping, Computation 7 (2019) 60, https://doi.org/10.3390/computation7040060.
[20] A.E. Galashev, K.A. Ivanichkina, Graphene and graphite supports for silicene stabilization: a computation study, J. Struct. Chem. 59 (4) (2018) 877–883, https://doi.org/10.1134/S0022476618040194.
[21] G.C. Fonseca, J.W. Handgraaf, E.J. Baerends, F.M. Bickelhaupt, Voronoi deformation density (VDD) charges: assessment of the Mulliken, Bader, Hirshfeld, Weinhold, and VDD methods for charge analysis, J. Comp. Chem. 25 (2) (2003) 189–210, https://doi.org/10.1002/jcc.10351.
[22] A.Y. Galashev, K.A. Ivanichkina, Silicene anodes for lithium-ion batteries on metal substrates, J. Electrochem. Soc. 167 (5) (2020) 050510, , https://doi.org/10.1149/1945-7111/ab717a.
[23] R. Hausbrand, G. Cherkashinin, H. Ehrenberg, M. Gröting, K. Albe, C. Hess, W. Jaegermann, Fundamental degradation mechanisms of layered oxide Li-ion battery cathode materials: Methodology, insights and novel approaches, Mater. Sci. Eng. B 192 (2015) 3–25, https://doi.org/10.1016/j.mseb.2014.11.014.
[24] W. Zhao, J. Yi, P. He, H. Zhou, Solid-state electrolytes for lithium-ion batteries: Fundamentals, challenges and perspectives, Electrochem. Energy Rev. 2 (2019) 574–605, https://doi.org/10.1007/s41918-019-00048-0.
[25] W. Rui, W. Shaofeng, W. Xiaozhi, Preprint The stability and charge carriers in bilayer silicene, arXiv:1305.4789v2 (21.05.2013).
[26] A.Y. Galashev, K.A. Ivanichkina, Computer test of a new silicene anode for lithium-ion batteries, ChemElectroChem 6 (5) (2019) 1525–1535, https://doi.org/10.1002/celc.201900119.
[27] A.Y. Galashev, K.A. Ivanichkina, Computer study of atomic mechanisms of intercalation/deintercalation of Li Ions in a silicene anode on an Ag (111) substrate, J. Electrochem. Soc. 165 (9) (2018) A1788–A1796, https://doi.org/10.1149/2.0751809jes.
[28] A.Y. Galashev, K.A. Ivanichkina, A.S. Vorob'ev, O.R. Rakhmanova, Structure and stability of defective silicene on Ag(001) and Ag(111) substrates: a computer experiment, Phys. Solid State 59 (6) (2017) 1242–1252, https://doi.org/10.1134/S1063783417060087.
[29] A.M. Nolan, Y. Liu, Y. Mo, Solid-state chemistries stable with high-energy cathodes for lithium-ion batteries, ACS Energy Lett. 4 (2019) 2444–2451, https://doi.org/10.1021/acsenergylett.9b01703.
[30] M. De Crescenzi, I. Berbezier, M. Scarselli, P. Castrucci, M. Abbarchi, A. Ronda, F. Jardali, J. Park, H. Vach, Formation of silicene nanosheets on graphite, ACS Nano 10 (2016) 11163–11171, https://doi.org/10.1021/acsnano.6b06198.
[31] J. Suk, D.Y. Kim, D.W. Kim, Y. Kang, Electrodeposited 3D porous silicon/copper films with excellent stability and high rate performance for lithium-ion batteries, J. Mater. Chem. A 2 (2014) 2478–2481, https://doi.org/10.1039/C3TA14645F.
[32] L. Tao, E. Cinquanta, D. Chiappe, C. Grazianetti, M. Fanciulli, M. Dubey, A. Molle, D. Akinwande, Silicene field-effect transistors operating at room temperature, Nat. Nanotechnol. 10 (3) (2015) 227–231, https://doi.org/10.1038/nnano.2014.325.
[33] Y. Cai, C.-P. Chuu, C.M. Wei, M.Y. Chou, Stability and electronic properties of two-dimensional silicene and germanene on graphene, Phys. Rev. B 88 (2013) 245408, , https://doi.org/10.1103/PhysRevB.88.245408.
[34] F. Banhart, J. Kotakoski, A.V. Krasheninnikov, Structural defects in graphene, ACS Nano 5 (2011) 26–41, https://doi.org/10.1021/nn102598m.
[35] G.R. Berdiyorov, F.M. Peeters, Influence of vacancy defects on the thermal stability of silicene: A reactive molecular dynamics study, RSC Adv. 4 (2014) 1133–1137, https://doi.org/10.1039/C3RA43487G.
[36] T. Sato, K. Komura, Method for splicing optical fibers having a plastic clad layer and an optical fiber suited for carrying out the method, Patent US4957343, 1990.
[37] X. Lu, G. Wu, J.W. Howard, A. Chen, Y. Zhao, L.L. Daemena, Q. Jia, Li-rich anti-perovskite Li3OCl films with enhanced ionic conductivity, Chem. Commun. 50 (2014) 11520–11522, https://doi.org/10.1039/C4CC05372A.
[38] H. Moon, H. Seong, W.C. Shin, W.-T. Park, M. Kim, S. Lee, J.H. Bong, Y.-Y. Noh, B.J. Cho, S. Yoo, S.G. Im, Synthesis of ultrathin polymer insulating layers by initiated chemical vapour deposition for low-power soft electronics, Nat. Mater. 14 (6) (2015) 628–635, https://doi.org/10.1038/nmat4237.
[39] T.P. Kaloni, M. Tahir, U. Schwingenschlög, Quasi free-standing silicene in a superlattice with hexagonal boron nitride, Sci. Rep. 3 (2013) 3192, https://doi.org/10.1038/srep03192.
[40] R. Quhe, R. Fei, Q. Liu, J. Zheng, H. Li, C. Xu, Z. Ni, Y. Wang, D. Yu, Z. Gao, J. Lu, Tunable and sizable band gap in silicene by surface adsorption, Sci. Rep. 2 (2012) 853, https://doi.org/10.1038/srep00853.
[41] X. Zhang, Z. Yu, S.-S. Wang, S. Guan, H.Y. Yang, Y. Yao, S.A. Yang, Theoretical prediction of MoN_2 monolayer as a high capacity electrode material for metal ion batteries, J. Mater. Chem. A 4 (2016) 15224–15231, https://doi.org/10.1039/C6TA07065E.
[42] F. Peymanirad, M. Neek-Amal, J. Beheshtian, F.M. Peeters, Graphene-silicene bilayer: A nanocapacitor with permanent dipole and piezoelectricity effect, Phys. Rev. B 92 (2015) 155113, , https://doi.org/10.1103/PhysRevB.92.155113.
[43] Z.H. Wang, M.J. Ni, Self-diffusion coefficient study of liquid lithium, Heat Mass Transfer 48 (2012) 253–257, https://doi.org/10.1007/s00231-011-0874-9.
[44] B. Peng, F. Cheng, Z. Tao, Lithium transport at silicon thin film: barrier for high-rate capability anode, J. Chen. Chem. Phys. 133 (2010) 034701, , https://doi.org/10.1063/1.3462998.
[45] J.F. Ribeiro, M. Silva, J. Carmo, L.M. Goncalves, M.M. Silva, J.H. Correia, Solid-State Thin-Film Lithium Batteries for Integration in Microsystems, in: B. Bhushan (Ed.), Scanning Probe Microscopy in Nanoscience and Nanotechnology, 3rd ed. Springer-Verlag, Berlin Heidelberg, 2013, pp. 575–619.
[46] J. Heon, J.W. Kim, Y.E. Sung, S.M. Oh, Failure modes of silicon powder negative electrode in lithium secondary batteries, Electrochem. Solid-State Lett. 7 (2004) A306–A309, https://doi.org/10.1149/1.1792242.
[47] Y. He, X. Yu, G. Li, R. Wang, H. Li, Y. Wang, H. Gao, Shape evolution of patterned amorphous and polycrystalline silicon microarray thin film electrodes caused by lithium insertion and extraction, J. Power Sources 216 (2012) 131–138, https://doi.org/10.1016/j.jpowsour.2012.04.105.
[48] X.H. Liu, L. Zhong, S. Huang, S.X. Mao, T. Zhu, J.Y. Huang, Sizedependent fracture of silicon nanoparticles during lithiation, ACS Nano 6 (2012) 1522–1531, https://doi.org/10.1021/nn204476h.
[49] J.Y. Li, Q. Xu, G. Li, Y.X. Yin, L.J. Wan, Y.G. Guo, Research progress regarding Si-based anode materials towards practical application in high energy density Li-ion batteries, Mater. Chem. Front. 1 (2017) 1691–1708, https://doi.org/10.1039/C6QM00302H.
[50] Q. Chen, R. Zhu, S. Liu, D. Wu, H. Fu, J. Zhu, H. He, Self-templating synthesis of silicon nanorods from natural sepiolite for high performance lithium-ion battery anodes, J. Mater. Chem. A 6 (2018) 6356–6362, https://doi.org/10.1039/C8TA00587G.
[51] P. Li, J.Y. Hwang, Y.K. Sun, Nano/microstructured silicon-graphite composite anode for high-energy-density Li-ion battery, ACS Nano. 13 (2019) 2624–2633, https://doi.org/10.1021/acsnano.9b00169.
[52] L. Zhang, C. Wang, Y. Dou, N. Cheng, D. Cui, Y. Du, P. Liu, M. Al-Mamun, S. Zhang, H. Zhao, A unique yolk-shell structured silicon anode with superior conductivity and high tap density for full Li-ion batteries, Angew Chem. 58 (2019) 8824–8828, https://doi.org/10.1002/ange.201903709.
[53] C.J. Zhang, S.H. Park, A. Seral-Ascaso, S. Barwich, N. McEvoy, C.S. Boland, J.N. Coleman, Y. Gogotsi, V. Nicolosi, High capacity silicon anodes enabled by MXene viscous aqueous ink, Nat. Commun. 10 (2019) 849, https://doi.org/10.1038/s41467-019-08383-y.
[54] S. Qi, X. Zhang, W. Lv, Y. Zhang, D. Kong, Z. Huang, Q.H. Yang, Electrode design from "internal" to "external" for high stability silicon anodes in lithium-ion batteries, ACS Appl. Mater. Interfaces 11 (2019) 14142–14149, https://doi.org/10.1021/acsami.9b02206.
[55] Y. Zhao, J. Wang, Q. He, J. Shi, Z. Zhang, X. Men, H. Yan Wang, Liions transport promoting and highly stable solid-electrolyte interface on Si in multilayer Si/C through thickness control, ACS Nano 13 (2019) 5602–5610, https://doi.org/10.1021/acsnano.9b00670.
[56] B. Wang, J. Ryu, S. Choi, X. Zhang, D. Pribat, X. Li, L. Zhi, S. Park, R.S. Ruoff, Ultrafast-charging silicon-based coral-like network anodes for lithium-ion batteries with high energy and power densities, ACS Nano 13 (2019) 2307–2315, https://doi.org/10.1021/acsnano.8b09034.
[57] J. Ma, J. Sung, J. Hong, S. Chae, N. Kim, S.H. Choi, G. Nam, Y. Son, S.Y. Kim, M. Ko, J. Cho, Towards maximized volumetric capacity via pore-coordinated design for large-volume-change lithium-ion battery anodes, Nat. Commun. 10 (2019) 475, https://doi.org/10.1038/s41467-018-08233-3.
[58] K.P.C. Yao, J.S. Okasinski, K. Kalaga, J.D. Almer, D.P. Abraham, Operando quantification of (de)lithiation behavior of silicongraphite blended electrodes for lithium-ion batteries, Adv. Energy Mater. 9 (2019) 1803380, https://doi.org/10.1002/aenm.201803380.